

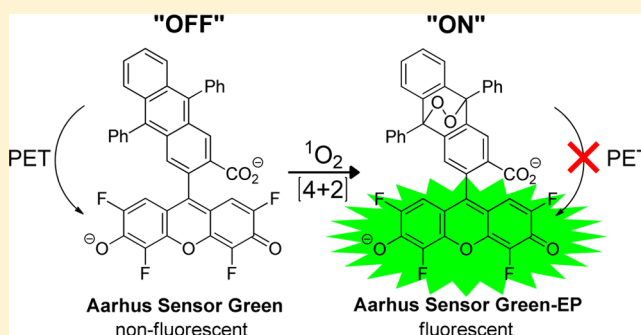
Aarhus Sensor Green: A Fluorescent Probe for Singlet Oxygen

Stephan K. Pedersen,[†] Jeppe Holmehave,[†] Frances H. Blaikie, Anita Gollmer, Thomas Breitenbach, Henrik H. Jensen, and Peter R. Ogilby*

Center for Oxygen Microscopy and Imaging, Department of Chemistry, Aarhus University, Langelandsgade 140, Aarhus 8000, Denmark

S Supporting Information

ABSTRACT: A tetrafluoro-substituted fluorescein derivative covalently linked to a 9,10-diphenyl anthracene moiety has been synthesized, and its photophysical properties have been characterized. This compound, denoted Aarhus Sensor Green (ASG), has distinct advantages for use as a fluorescent probe for singlet molecular oxygen, $O_2(a^1\Delta_g)$. In the least, ASG overcomes several limitations inherent to the use of the related commercially available product called Singlet Oxygen Sensor Green (SOSG). The functional behavior of both ASG and SOSG derives from the fact that these weakly fluorescent compounds rapidly react with singlet oxygen via a $\pi^2 + \pi^4$ cycloaddition to irreversibly yield a highly fluorescent endoperoxide. The principal advantage of ASG over SOSG is that, at physiological pH values, both ASG and the ASG endoperoxide (ASG-EP) do not themselves photosensitize the production of singlet oxygen. As such, ASG better fits the requirement of being a benign probe. Although ASG readily enters a mammalian cell (i.e., HeLa) and responds to the presence of intracellular singlet oxygen, its behavior in this arguably complicated environment requires further investigation.



INTRODUCTION

Over the years, a great effort has gone into the design, synthesis, and characterization of fluorescent probes for reactive oxygen species (ROS), particularly for use in functional biological systems (e.g., a live cell).^{1–5} ROS of interest in this regard include hydrogen peroxide, the hydroxyl radical, the superoxide ion ($O_2^{\bullet-}$), and singlet molecular oxygen ($O_2(a^1\Delta_g)$). These small molecules can diffuse and react with other molecules (e.g., proteins, lipids, DNA) and thereby influence the behavior of both plant and mammalian cells. ROS are a part of normal cell signaling and function; they play a key role in cell maintenance, cell death, and the response of cells to perturbations.⁶ Understanding the production, behavior, and effects of ROS in cells and organisms is important with respect to processes of aging, effectiveness of drugs, and mechanisms of biological defense.⁶

We have been particularly interested in monitoring and characterizing the behavior of $O_2(a^1\Delta_g)$, which is the lowest excited electronic state of molecular oxygen.⁷ $O_2(a^1\Delta_g)$ can be generated in many ways pertinent to cellular biology. These include inherent enzymatic and stress-response processes,^{8,9} as well as photosensitized processes wherein a photoexcited electronic state of a given molecule (the sensitizer) transfers its energy of excitation to the triplet ground state of oxygen, $O_2(X^3\Sigma_g^-)$.^{10,11} $O_2(a^1\Delta_g)$ is also often involved in processes that result in the production of other ROS.^{6,12} $O_2(a^1\Delta_g)$ uniquely reacts with many organic and bio-organic molecules¹³ and thereby plays a role in mechanisms of cell signaling and, at

the limit, in events that perturb cell homeostasis and result in cell death.^{9,14}

Although $O_2(a^1\Delta_g)$ is arguably best detected using its characteristic $O_2(a^1\Delta_g) \rightarrow O_2(X^3\Sigma_g^-)$ phosphorescence at 1275 nm, particularly in time-resolved experiments, this is a challenging endeavor in many biological systems.^{11,15,16} Specifically, the quantum yield of $O_2(a^1\Delta_g)$ phosphorescence under these conditions is generally $<10^{-6}$. This is compounded by the fact that the pertinent concentrations of $O_2(a^1\Delta_g)$ involved are invariably small (i.e., $<10^{-6}$ M). As such, the amount of $O_2(a^1\Delta_g)$ to be detected in a typical single cell imaging experiment is miniscule. Lastly, IR detectors used to monitor the 1275 nm phosphorescence are not as efficient as the detectors used to monitor corresponding optical signals in the visible region of the spectrum. All of this reinforces the importance of alternative methods for monitoring $O_2(a^1\Delta_g)$. To this end, much recent work has been done on developing and characterizing biologically compatible molecules that yield a clear optical signal in the visible region of the spectrum (e.g., increase in fluorescence intensity) upon reaction with $O_2(a^1\Delta_g)$.^{17–27}

One fluorescent probe for $O_2(a^1\Delta_g)$ that has received recent attention is the so-called Singlet Oxygen Sensor Green (SOSG), Figure 1. This is a commercially available product²⁸ that is based on a successful two-component paradigm in which a $O_2(a^1\Delta_g)$ trapping moiety (a substituted anthracene) is

Received: January 28, 2014

Published: March 7, 2014



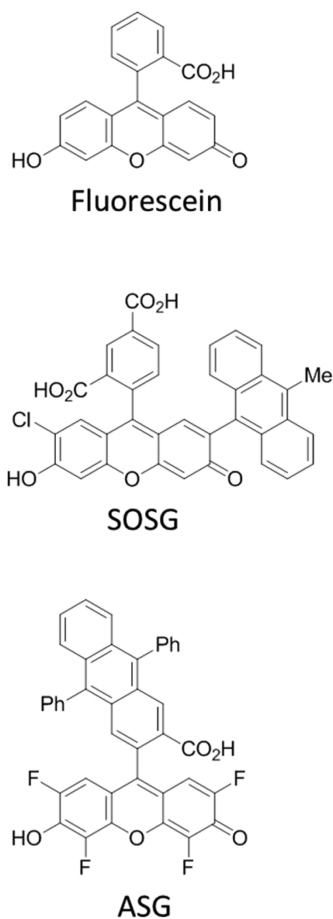


Figure 1. Structures for uncharged forms of fluorescein, Singlet Oxygen Sensor Green (SOSG), and Aarhus Sensor Green (ASG).

coupled to a light-emitting chromophore (a fluorescein derivative).¹⁷ Prior to the reaction with $O_2(a^1\Delta_g)$, emission from the chromophore is quenched by electron transfer from the trapping moiety; the probe is in the “off” position. Upon reaction with $O_2(a^1\Delta_g)$, however, the resultant oxygen adduct (an anthracene endoperoxide) is no longer an efficient intramolecular electron donor, and light emission from the fluorescein moiety occurs; the probe is now switched “on”.

Although SOSG has many attractive features, we have recently shown that its use can be adversely affected because the oxygen adduct (i.e., the SOSG endoperoxide, denoted SOSG-EP) is itself a good $O_2(a^1\Delta_g)$ sensitizer.²⁴ Specifically, the fluorescein-related chromophore in SOSG-EP photo-sensitizes the production of $O_2(a^1\Delta_g)$ with a quantum yield as large as 0.2. Thus, upon irradiating the SOSG system to probe for the presence of $O_2(a^1\Delta_g)$, one also makes an appreciable amount of $O_2(a^1\Delta_g)$ in the process. This is clearly an undesirable feature.

For the present study, we set out to ascertain whether judicious chemical modification of the fluorescein-derived chromophore in SOSG could yield a molecule that itself does not produce $O_2(a^1\Delta_g)$ and, as such, gives rise to a better probe for $O_2(a^1\Delta_g)$. In our view, it is advantageous to retain the connection to fluorescein simply because there is already a great deal known about modulating the properties of this molecule for use as a fluorescence probe.^{29–34} With this previous work in mind, we examined the characteristics of SOSG derivatives in which the fluorescein-derived chromo-

phore was selectively fluorinated, much like the dyes Oregon Green³³ and Pennsylvania Green,³¹ which are fluorinated derivatives of fluorescein-based fluorescent probes. We now report that a tetrafluoro-substituted fluorescein derivative covalently linked to a 9,10-diphenyl anthracene moiety, denoted Aarhus Sensor Green (ASG), Figure 1, overcomes the principal disadvantage of SOSG. Specifically, ASG and the ASG endoperoxide do not sensitize the production of $O_2(a^1\Delta_g)$ at physiologically pertinent pH values of ~ 7 .

RESULTS AND DISCUSSION

1. Design of Aarhus Sensor Green. Outlined below in successive sections are points that were considered in the design of ASG.

1.1. pH Dependence of $O_2(a^1\Delta_g)$ Production by Fluorescein Derivatives. It is well established that the fluorescence quantum yield of fluorescein depends on the pH of the medium in which this molecule is dissolved.^{31,33,34} Specifically, at pH ~ 4 where the molecule exists as shown in Figure 1, the fluorescence is comparatively weak. However, under alkaline conditions where the molecule exists as the dianion (i.e., carboxylate and phenolate), the fluorescence quantum yield increases appreciably. The pK_a of neutral fluorescein is ~ 4.2 (yields the carboxylate), and the pK_a of the monoanion is ~ 6.5 (yields the phenolate).³³

We have independently established that the pH dependence of the fluorescein-sensitized $O_2(a^1\Delta_g)$ yield complements the pH-dependent fluorescence quantum yields.²⁴ Specifically, under acidic conditions where fluorescein does not appreciably fluoresce, the $O_2(a^1\Delta_g)$ quantum yield, ϕ_Δ , is comparatively large (e.g., $\phi_\Delta = 0.2$ at pD 3.2). However, under alkaline conditions where fluorescein is highly fluorescent, the $O_2(a^1\Delta_g)$ yield drops considerably (e.g., $\phi_\Delta = 0.02$ at pD 10.7). This is illustrated in Figure 2. [In this earlier publication, ref 24, we

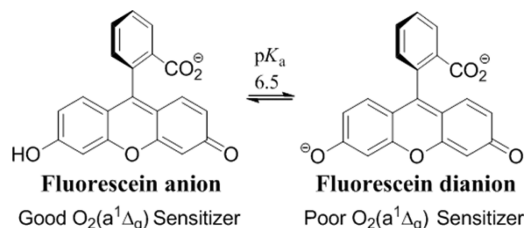
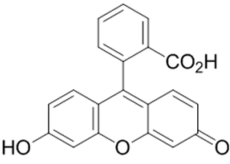
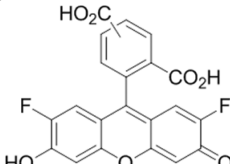
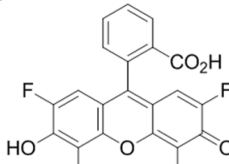


Figure 2. Illustration of the pH-dependent change in fluorescein that influences the yield of sensitized $O_2(a^1\Delta_g)$ production. Note also that, as a consequence of the carboxylate group, the π system of the pendant benzoic acid is not coplanar with the π system of the xanthene-derived moiety in fluorescein. The latter defines the principal chromophore in this molecule.

incorrectly referred to pH instead of pD values. These $O_2(a^1\Delta_g)$ experiments were performed in D_2O instead of H_2O to exploit the fact that the lifetime of $O_2(a^1\Delta_g)$ is appreciably longer in D_2O than in H_2O , and consequently, the quantum efficiency of $O_2(a^1\Delta_g)$ phosphorescence is greater in D_2O .^{10,35} Note that $pD = pH + 0.4$).^{36]}

With the above-mentioned pH-dependent fluorescence and $O_2(a^1\Delta_g)$ data in mind and the desire to develop a $O_2(a^1\Delta_g)$ probe that can be used in biological media, it is clear that one goal will be to functionalize the fluorescein-derived moiety in such a way as to reduce the pK_a values and thereby create a poorer $O_2(a^1\Delta_g)$ sensitizer. We can carry this point one step further and assume that the pertinent functional group in this

Table 1. Quantum Yields of $O_2(a^1\Delta_g)$ Production Photosensitized using Fluorinated Derivatives of Fluorescein^a

 Fluorescein		 Carboxy Oregon Green ^b		 4',5'-Difluoro-Oregon Green	
pD ^c	ϕ_Δ	pD	ϕ_Δ	pD	ϕ_Δ
3.2	0.21	4.0	0.20	4.4	0.04
7.1	0.14	7.3	0.04	7.6	0.06
10.7	0.02	9.0	0.02	10.2	0.07

^aExperiments were performed in D_2O to capitalize on the fact that the $O_2(a^1\Delta_g)$ lifetime and hence $O_2(a^1\Delta_g)$ phosphorescence intensity are greater in D_2O than in H_2O . Errors on the ϕ_Δ values are $\sim \pm 10\%$. ^bWe used a mixture of the 5- and 6-carboxy Oregon Green.³³ ^cIn our earlier report on fluorescein,²⁴ we incorrectly indicated that the ϕ_Δ values were recorded at selected pH values. As correctly indicated here, they were recorded at selected pD values in D_2O .

regard is the phenol on the chromophore itself (Figure 2). To this end, we set out to examine the effects of fluorinating the xanthene-related moiety in fluorescein (Table 1).

The data obtained show that upon increasing the extent of fluorination of the chromophore in fluorescein, one can indeed reduce the photosensitized yield of $O_2(a^1\Delta_g)$ production under neutral and acidic conditions. This is consistent with the expectation that (a) we have indeed reduced the pK_a value of the phenol functional group with the introduction of the electron-withdrawing groups and (b) the dianion form of fluorescein is not an efficient $O_2(a^1\Delta_g)$ sensitizer.

On the basis of independent studies performed over the years, it is indeed reasonable to expect that the phenolate form of fluorescein (the dianion) would be a poorer $O_2(a^1\Delta_g)$ sensitizer than the phenol form of fluorescein (the anion, Figure 2). Specifically, it has been established that molecules which can more readily donate an electron to oxygen in the excited state encounter complex (that necessarily precedes the formation of $O_2(a^1\Delta_g)$) tend to be poorer sensitizers of $O_2(a^1\Delta_g)$. In short, increasing the extent to which the $Sens^+ \cdot O_2^-$ charge-transfer state plays a role in the encounter complex is known to adversely affect the energy transfer process that results in $O_2(a^1\Delta_g)$.^{10,11,37–42} From ground-state experiments, it is known that the phenoxide anion (i.e., the fluorescein dianion) is more readily oxidized than the corresponding phenol.⁴³ The latter readily extends to the corresponding excited states.

Thus, if we indeed retain the fluorescein-derived moiety as our fluorophore in the development of a new $O_2(a^1\Delta_g)$ probe, the use of a tetrafluorinated derivative will be to our benefit in that we would then appreciably reduce the yield of $O_2(a^1\Delta_g)$ sensitized by the probe itself.

1.2. $O_2(a^1\Delta_g)$ Trapping Moiety. In looking at the structure of SOSG (Figure 1) and upon considering the data in Table 1, it will likely be best if the anthracene moiety used to trap $O_2(a^1\Delta_g)$ is attached to the xanthene-related moiety at the position normally occupied by the benzoic acid group in fluorescein. In this way, we can more readily accommodate the introduction of four fluorine substituents on the chromophore/fluorophore.

Of course, such a direct substitution best facilitates the required electron transfer from the anthracene group to the xanthene group that keeps the probe in the “off” position (i.e., the electron transfer reaction from the anthracene that quenches the emissive xanthene excited state). Moreover, in making this substitution, it will be important to ensure that the favored conformation of the molecule will position the anthracene π system such that it is orthogonal to the π system of the operative chromophore/fluorophore.^{17,22} This latter stipulation ensures that, with the exception of the desired changes in the electron transfer reaction, the xanthene-related chromophore/fluorophore acts independently of changes in the extent of conjugation in the anthracene moiety as $O_2(a^1\Delta_g)$ is trapped. The introduction of a carboxyl group in the 2 position of the anthracene moiety would accomplish this goal (see Figure 2).^{17,22}

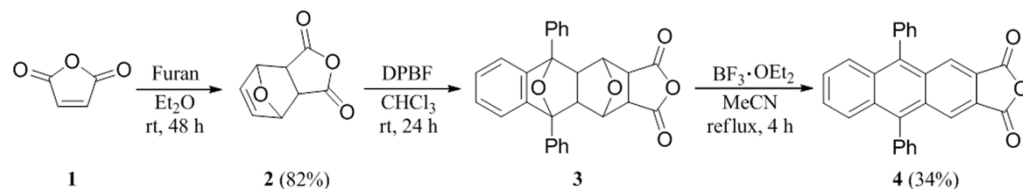
Finally, it is necessary to consider the effective nucleophilicity of the anthracene moiety with respect to the desired $\pi 2 + \pi 4$ reaction with $O_2(a^1\Delta_g)$; an electron-rich anthracene will react much faster with $O_2(a^1\Delta_g)$.⁴⁴ Although a number of options are available in this regard, we chose to start our investigations with a diphenyl substituted anthracene.

In this way, we arrived at the target molecule for this study shown in Figure 1 and denoted this ASG. It is important to note in this regard that ASG is a tetrafluorinated analogue of a molecule, denoted DPAX, that has been synthesized and studied by Nagano and his collaborators (DPAX = 9-[2-(3-carboxy-9,10-DiPhenyl)Anthryl]-6-hydroxy-3H-Xanthen-3-one).^{17,45}

2. Synthesis of Aarhus Sensor Green. In synthesizing ASG, we followed the basic principles used by Nagano and colleagues⁴⁵ in the synthesis of DPAX. As outlined below, however, minor modifications were made in the procedure that facilitated simplicity and increased product yields.

The appropriate 9,10-diphenyl anthracyl reactant, **4**, was prepared as outlined in Scheme 1 using a procedure published by Donyagina et al. (DPBF = 1,3-diphenylisobenzofuran).⁴⁶ Using this approach, we obtained the anhydride **4** in an overall yield of 28%. In contrast, Nagano and colleagues⁴⁵ obtained the

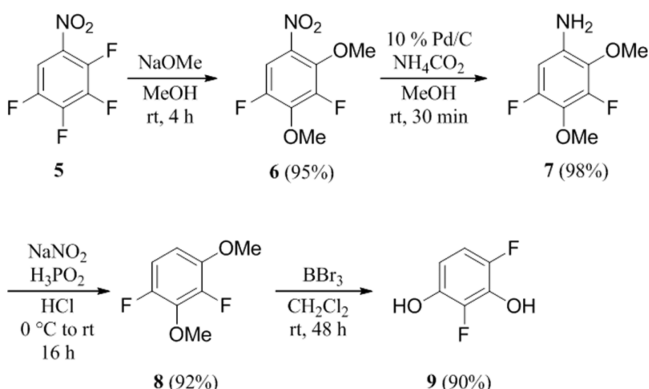
Scheme 1



same compound in 9% yield using a more convoluted approach.

For the synthesis of DPAX, the anhydride **4** was then condensed with resorcinol to yield the desired product in 43% yield.⁴⁵ In our case, to synthesize ASG, the analogous procedure would involve the use of 2,4-difluoresorcinol (**9**). We prepared **9** in 90% overall yield using the procedure of Sun et al.³³ (Scheme 2).

Scheme 2



To conclude and prepare ASG, we first tried to condense the difluoresorcinol **9** with the anhydride **4** using the reaction conditions of Nagano and colleagues.⁴⁵ However, the presence of the two fluorines appears to decrease the nucleophilicity of the resorcinol; we were unable to detect appreciable formation of the expected ASG product when the condensation was carried out for 24 h at 80 °C in MeSO₃H. Rather, we needed to increase the reaction temperature to 150 °C before ASG formation could be observed using ¹⁹F NMR (Scheme 3).

Although the condensation reaction between **9** and **4** in MeSO₃H yields ASG, the isolation and purification of ASG was facilitated using the protocol of Sun et al.,³³ in which we treated the initial product mixture with acetic anhydride in pyridine to form a mixture containing the lactone **10** (Scheme 3). We chromatographed this latter mixture containing **10** on a silica gel column, deacetylated the resultant material with ammonia, and then used reverse-phase MPLC to obtain pure ASG in 12% yield from **9** and **4**.

3. Characterization of Aarhus Sensor Green's Photochemistry. The absorption and emission spectra of ASG in D₂O (Figure 3) are consistent with and similar to spectra recorded from other fluorescein derivatives,^{31,33,45} including SOSG.^{20,24} The absorption bands in the range ~350–450 nm arise from the diphenyl anthracene moiety, whereas the band with a maximum at 510 nm and extinction coefficient of $(2.3 \pm 0.2) \times 10^4 \text{ cm}^{-1} \text{ M}^{-1}$ is assigned to the fluorescein moiety. However, this extinction coefficient for ASG is smaller than the value of $7.8 \times 10^4 \text{ cm}^{-1} \text{ M}^{-1}$ reported by Sun et al.³³ for a

Scheme 3

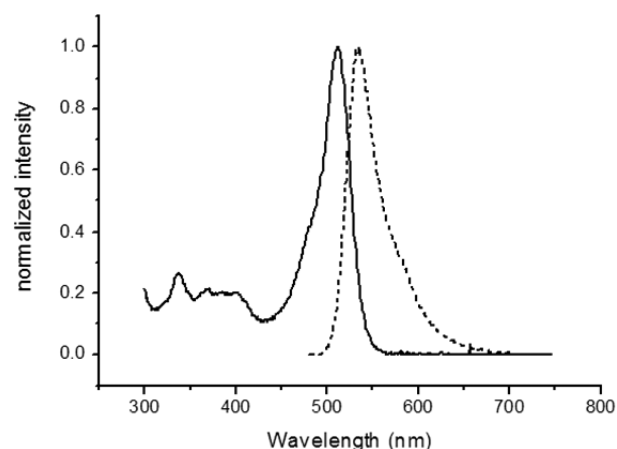
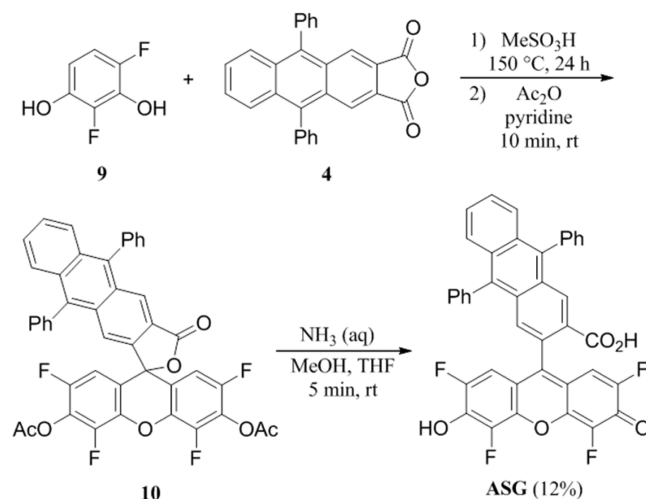


Figure 3. Normalized absorption (solid line) and fluorescence (dotted line) spectra of ASG in unbuffered D₂O (i.e., pD ~ 7).

corresponding tetrafluorinated derivative of fluorescein. The fluorescence band of ASG has a maximum at 537 nm in D₂O.

Using an independent solution of fluorescein in alkaline D₂O as a fluorescence standard ($\phi_f = 0.98 \pm 0.01$),⁴⁷ we ascertained that the quantum efficiency of fluorescence from ASG in pD ~ 7 D₂O was 0.04 ± 0.01 . Although this number is sufficiently small for use as an “off → on” fluorescence probe, it is nevertheless slightly larger than the corresponding value we recorded from SOSG ($\phi_f = 0.009 \pm 0.001$).²⁴ In any event, in many cases it is useful to be able to monitor some fluorescence from the probe when in the “off” condition (e.g., to define probe location in imaging applications in heterogeneous media).

The data shown in Figure 4 address the principal point of this study and clearly demonstrate that, with ASG, we have indeed overcome the main limitation of using SOSG. We first show that, upon irradiating a known O₂(^{a1}Δ_g) sensitizer

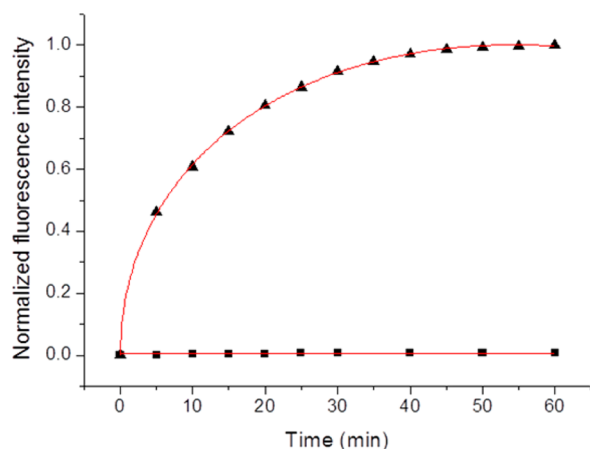


Figure 4. Fluorescence intensity of D₂O solutions containing ASG recorded at 537 nm as a function of elapsed irradiation time under two different conditions. The data shown as triangles were recorded upon irradiation of a codissolved O₂(a¹Δ_g) sensitizer and show the expected/desired response to the presence of O₂(a¹Δ_g). The data shown as squares were recorded upon irradiation of ASG at 420 nm and likewise show the desired response. The lines superimposed on the data are meant simply as guides to the eye.

(phenalene-1-one-2-sulfonic acid with $\phi_{\Delta} = 1.0$) codissolved with ASG, the intensity of the sample's fluorescence at 537 nm increases appreciably (triangles in Figure 4). This is the expected result as a consequence of the photosensitized production of O₂(a¹Δ_g) and the subsequent reaction of O₂(a¹Δ_g) with ASG to yield the ASG endoperoxide (ASG-EP). The data show asymptotic behavior simply because, under our experimental conditions, we consume all of the ASG in solution over the elapsed irradiation period to yield ASG-EP. We ascertained that the quantum efficiency of fluorescence of ASG-EP is 0.4 ± 0.04 .

Most importantly, upon irradiating a D₂O solution of ASG at 420 nm, we find that the fluorescence intensity of the system at 537 nm does not increase over the elapsed period of irradiation (squares in Figure 4). In short, irradiation of ASG itself does not give a positive response for O₂(a¹Δ_g). The irradiation wavelength of 420 nm was chosen simply because many O₂(a¹Δ_g) photosensitized experiments are performed using light of this wavelength.²⁴ In contrast, upon irradiating SOSG under these same conditions, the intensity of the detected fluorescence increases appreciably, demonstrating that SOSG and SOSG-EP themselves sensitize the production of O₂(a¹Δ_g).^{20,24} In support of the data shown in Figure 4, upon prolonged laser irradiation of ASG in D₂O (3 h at 420 nm with 3 mW, pD ~7), we were never able to detect (1) a O₂(a¹Δ_g) phosphorescence signal at 1275 nm and (2) the production of ASG-EP. Given our limits for detecting O₂(a¹Δ_g) by its 1275 nm phosphorescence, we can thus state that $\phi_{\Delta} < 0.02$ for ASG and/or ASG-EP. Under corresponding conditions with the SOSG system, we detected a O₂(a¹Δ_g) phosphorescence signal and ascertained that SOSG-EP produces O₂(a¹Δ_g) with a quantum yield of 0.18 ± 0.02 .²⁴ As we have already indicated,²⁴ it is the fluorescein-related chromophore in SOSG-EP that is the O₂(a¹Δ_g) sensitizer.

To reinforce our conclusion regarding ASG, we performed a series of independent experiments using 510 nm irradiation (i.e., the wavelength that corresponds to the absorption band maximum of the tetrafluoro fluorescein derivative in ASG, see Figure 3), monitoring emission from the sample at 1275 nm

(i.e., O₂(a¹Δ_g) phosphorescence). The data recorded upon irradiation of ASG and ASG-EP, independently, were identical (Figure 5); we were not able to record a O₂(a¹Δ_g)

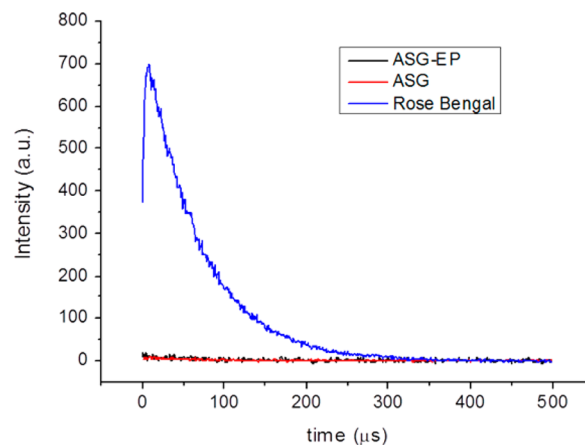


Figure 5. Time-resolved emission data recorded at 1275 nm. The trace shown in blue was recorded upon 510 nm irradiation of a D₂O solution of Rose Bengal, which is an established O₂(a¹Δ_g) sensitizer (for the data shown, absorbance at 510 nm = 0.1). The data correspond to the expected O₂(a¹Δ_g) phosphorescence signal. The traces shown in red and black were recorded upon 510 nm irradiation of D₂O solutions of ASG and ASG-EP, respectively (absorbance at 510 nm of 0.1 and 0.4, respectively).

phosphorescence signal in either case. As a control experiment, we irradiated a corresponding D₂O solution of Rose Bengal, which is an established O₂(a¹Δ_g) sensitizer ($\phi_{\Delta} = 0.76 \pm 0.02$).⁴⁸ In this case, the expected O₂(a¹Δ_g) phosphorescence signal was observed.

In another independent experiment, O₂(a¹Δ_g) was produced upon irradiation of the known sensitizer phenalene-1-one-2-sulfonic acid, and we monitored O₂(a¹Δ_g) phosphorescence in time-resolved experiments as a function of the amount of codissolved ASG. Quantifying the effect of added ASG on the lifetime of O₂(a¹Δ_g) through a 6-point Stern–Volmer plot yielded a rate constant for ASG-mediated O₂(a¹Δ_g) removal/deactivation of $(1.7 \pm 0.1) \times 10^7 \text{ s}^{-1} \text{ M}^{-1}$. Although this number is larger than what has been observed for 9,10-diphenyl anthracene in nonpolar solvents ($\sim 1 \times 10^6 \text{ s}^{-1} \text{ M}^{-1}$),⁴⁴ it is well within reason for this type of a reaction. Indeed, this rate constant is large enough to make ASG a viable probe for O₂(a¹Δ_g) in many systems. Carrying this latter point further, we have also determined that ASG does not react with two other common ROS: the superoxide ion and H₂O₂. Specifically, upon the addition of potassium superoxide or H₂O₂ (successive aliquots of a 33% solution of H₂O₂) to an aqueous solution at pD ~7 containing ASG, we did not see an increase in fluorescence intensity at 537 nm or evidence of ASG degradation.

4. Aarhus Sensor Green in Mammalian Cells. Although SOSG is marketed as a cell-impermeable compound,²⁸ we have ascertained that there are incubating conditions in which it can be readily incorporated into a mammalian cell.²⁴ We also ascertained that the photophysics and photochemistry of intracellular SOSG appears to differ appreciably from that of SOSG in vitro, and more work needs to be done to better characterize the behavior of SOSG as a probe for O₂(a¹Δ_g) in biological systems.²⁴ These statements about SOSG are equally applicable to ASG.

ASG can likewise be readily incorporated into a mammalian cell (Figure 6). As with SOSG,²⁴ the specific procedure involves

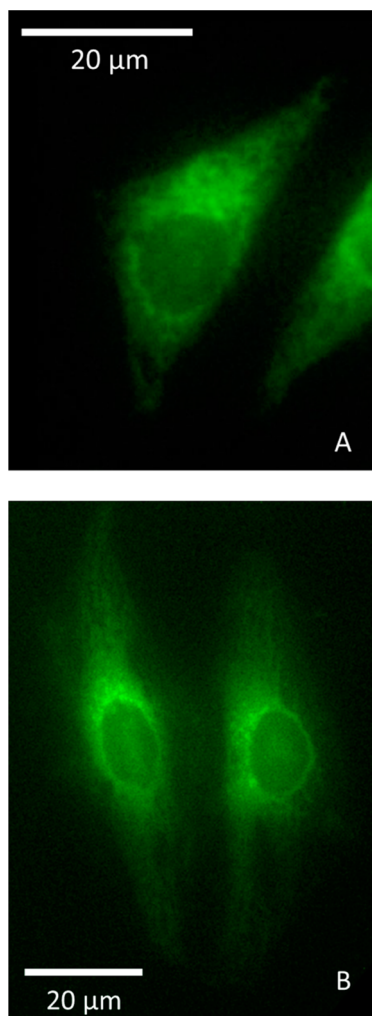


Figure 6. Images of HeLa cells based on the fluorescence of ASG. The darker round spot in the center of each cell is the nucleus. (A) Cells that had been incubated with ASG alone. (B) Cells containing ASG and the $O_2(a^1\Delta_g)$ sensitizer PpIX.

the use of an incubating medium that lacks added proteins. The available evidence indicates that, like SOSG, ASG binds to the proteins in the medium and this, in turn, inhibits uptake by the cell.²⁴

Although ASG can be put into a cell, the specific site of intracellular localization also appears to depend on the experimental conditions. For example, upon incubating HeLa cells with a protein-free medium containing ASG, we find that ASG tends to localize in “clumps” in the extra-nuclear cytoplasm (Figure 6A). However, under incubating conditions that also include S-aminolevulinic acid, ALA, which is a precursor for the intracellular biosynthetic production of the $O_2(a^1\Delta_g)$ sensitizer protoporphyrin IX, PpIX,⁴⁹ we find that ASG tends to localize in strand-like structures (Figure 6B). The latter are often associated with and characteristic of mitochondria that are bound to cytoskeletal proteins.^{50–53}

Upon the photosensitized production of intracellular $O_2(a^1\Delta_g)$, we were indeed able to see an increase in the intensity of fluorescence at 530–540 nm from cells that had been incubated with ASG. However, this increase in

fluorescence intensity was observed upon irradiation of some $O_2(a^1\Delta_g)$ sensitizers (pyropheophorbide *a*) but was not observed upon irradiation of other $O_2(a^1\Delta_g)$ sensitizers (PpIX). This result is arguably expected given that ASG and a given sensitizer can localize in different intracellular domains, and given the intracellular lifetime and diffusion coefficient of $O_2(a^1\Delta_g)$, the $O_2(a^1\Delta_g)$ produced in one place may be deactivated/react before it reaches ASG in a second place.^{15,54,55}

In light of the points mentioned above, more work clearly needs to be done to fully characterize the behavior and response of ASG in cells. Issues that specifically need to be addressed include (1) $O_2(a^1\Delta_g)$ -mediated changes in the intracellular location of both ASG and ASG-EP and (2) the binding of ASG and/or ASG-EP to selected proteins. Phenomena such as these can appreciably alter the photo-physics of the system, particularly the fluorescence signal monitored.²⁴ Once these fundamental issues are better elucidated, it will be possible to systematically address the important inference (*vide supra*) regarding the intracellular locations of ASG and a given $O_2(a^1\Delta_g)$ sensitizer, correlating the results to the intracellular diffusion distance and lifetime of $O_2(a^1\Delta_g)$. These latter studies clearly fall under the category of using ASG as a tool to probe the intracellular behavior of $O_2(a^1\Delta_g)$.

One obvious requirement of an intracellular probe for $O_2(a^1\Delta_g)$ is that the molecule itself is not cytotoxic. We first ascertained that, in the absence of light, ASG indeed does not adversely influence HeLa cells (Figure 7). On the contrary,

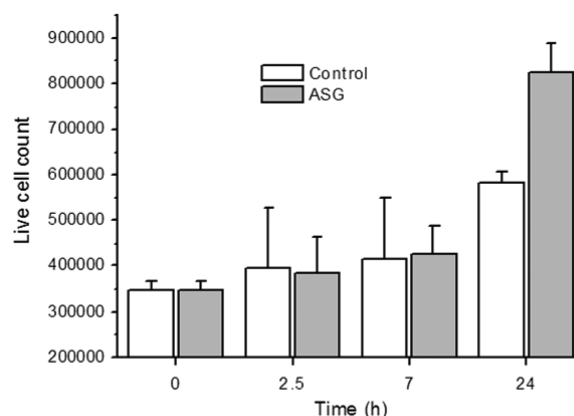


Figure 7. Number of live HeLa cells in a given culture as a function of the incubation time after intracellular incorporation of ASG. The time period of incubating the cells in a medium containing 1 μ M ASG was 2 h. At this point, the cells were washed, and the extracellular ASG was removed. Thus, the data recorded at $t = 2.5$ h arguably represents the starting point of this experiment. The control sample (nonshaded pylon) represents a cell culture not exposed to ASG.

within the error limits of our measurements, one could even claim that ASG stimulates cell proliferation (Figure 7). However, the key feature that sets ASG apart from SOSG is its effect, or lack thereof, on cells in the presence of light. Irradiation of intracellular SOSG ultimately results in an adverse effect on the cell; we observe morphological signs characteristic of cell death. This is to be expected given that SOSG photosensitizes the production of $O_2(a^1\Delta_g)$,²⁴ and the latter is cytotoxic in large amounts.^{14,50} On the other hand, upon prolonged irradiation of intracellular ASG, we did not observe corresponding adverse effects on the cell. Again, this is

to be expected given that ASG does not sensitize the production of $O_2(a^1\Delta_g)$ in appreciable yield (or rather, it appears that the in vitro result regarding the ASG photosensitized yield of $O_2(a^1\Delta_g)$ carries over to the cell experiments).

CONCLUSIONS

We find that for fluorescein-based fluorescence probes of $O_2(a^1\Delta_g)$, adding fluorine atoms to the chromophore/fluorophore decreases the efficiency with which this chromophore/fluorophore sensitizes the production of $O_2(a^1\Delta_g)$ at physiological pH. This is clearly a desired characteristic of a probe for $O_2(a^1\Delta_g)$. This approach was realized in the synthesis of ASG, which is a two-component system consisting of a tetrafluoro fluorescein derivative coupled to a 9,10-diphenyl anthracene moiety which acts as the $O_2(a^1\Delta_g)$ trap. In this regard, ASG overcomes one limitation of the structurally related and commercially available fluorescent probe for $O_2(a^1\Delta_g)$, SOSG. Although ASG is readily incorporated into a mammalian cell and is not cytotoxic, more work needs to be done to fully characterize its behavior and response to intracellular $O_2(a^1\Delta_g)$.

EXPERIMENTAL SECTION

Instrumentation and Methods. The instrumentation and methods used to monitor $O_2(a^1\Delta_g) \rightarrow O_2(X^3\Sigma_g^-)$ phosphorescence at ~ 1275 nm in time-resolved experiments and to quantify photosensitized $O_2(a^1\Delta_g)$ quantum yields and $O_2(a^1\Delta_g)$ lifetimes have been described.^{56–58} All $O_2(a^1\Delta_g)$ experiments were performed in 1 cm path length cuvettes. For the fluorescence quantum yield measurements, the sample absorbance in 1 cm path length cells did not exceed 0.05.

Although general features of our cell imaging experiments have likewise been described,^{55,59} some changes were incorporated for the present study. Briefly, the fluorescence-based images of HeLa cells were obtained after incubation for 2 h in a buffered protein-free medium^{24,60} containing 1 μ M ASG. The cells were then washed twice with an ASG-free medium and mounted on the stage of an inverted microscope. The images were recorded by irradiating the entire cell and its surroundings with the output of a steady-state 200 W metal-halide lamp. A band-pass filter centered at 500 nm (10 nm fwhm) was used to isolate the excitation wavelength, and a band-pass filter centered at 540 nm (10 nm fwhm) was used to isolate emission from the sample. The excitation light was directed to the sample using a FITC-dichroic mirror, and the images were obtained using a CCD camera. The system was controlled using the program μ Manager.⁶¹

Incorporation of PpIX into HeLa cells was achieved by incubating the cells for 2 h with ALA (1 mM, Sigma) in normal growth medium. The medium was then replaced with the above-mentioned protein-free medium containing 1 μ M ASG and 1 mM ALA, and incubation proceeded for an additional 2 h.

For the cytotoxicity study (Figure 7), HeLa cells were seeded after trypsinization into a 25 cm² flask with a cell density of ca. 8000 cells/cm². The culture was left overnight in a 5% CO₂ incubator to establish controlled growth conditions. The next day, the cell number for the start (i.e., 0 h in Figure 7) was determined in two independent samples. In other flasks, the culture medium was removed and replaced by a protein-free medium (control) and, independently, a protein-free medium containing 1 μ M ASG. After 2 h, the media was removed from all flasks, and the cultures were washed twice with ASG-free medium. Normal growth medium was added to all flasks, and the cultures were placed back into the incubator. Cell counts were performed after trypsinization (0.25% trypsin in EDTA (~ 0.5 mM), Sigma) in a hemocytometer at the time points 2.5, 7, and 24 h after the incubation start. All steps were performed under red light ($\lambda > 600$ nm) to avoid cell damage induced by light.

Materials. Chemicals for the Photophysical Studies. Phenalene-1-one-2-sulfonic acid was synthesized according to a published method.⁶² Fluorescein (95%, Sigma Aldrich) and D₂O (>99.9% D, Euriso-Top) were used as received. The mixture of 5- and 6-carboxy Oregon Green and 4',5'-difluoro-Oregon Green were synthesized using the general procedure of Sun et al.³³ and given to us as a gift by Mikkel Due Petersen.

Synthesis of ASG. General Methods. All purchased chemicals were used as received without further purification. Solvents were dried according to standard procedures, and flash chromatography was carried out on silica gel 60 (230–400 mesh). The chemical shifts are reported in ppm relative to the solvent residual peak. The ¹H NMR spectra were recorded at 400 MHz, ¹³C NMR spectra at 100 MHz, ¹⁹F NMR spectra at 377 MHz. MS spectra were recorded on a LC-TOF (ES) apparatus.

3a,4,7,7a-Tetrahydro-4,7-epoxyisobenzofuran-1,3-dione (2). Furan (1.4 mL, 20.4 mmol) and maleic anhydride (2.00 g, 20.4 mmol) were dissolved in diethyl ether (5.0 mL) and stirred for 48 h at room temperature. A white precipitate formed and was collected by filtration and recrystallized from acetone to yield pure 3a,4,7,7a-tetrahydro-4,7-epoxyisobenzofuran-1,3-dione (2) as a white solid (2.78 g, 16.7 mmol, 82%). ¹H NMR (400 MHz, CDCl₃): δ_H ppm 6.58 (s, 2H), 5.46 (s, 2H), 3.17 (s, 2H). ¹³C NMR (100 MHz, CDCl₃): δ_C ppm 169.8, 137.0, 82.2, 48.7. HRMS: [M + H]⁺ calcd for C₈H₆O₄, 167.0344; found, 167.0352. Our data are in accord with previously reported data.⁶³

9,10-Diphenylanthra[2,3-c]furan-1,3-dione (4). 1,3-Diphenylisobenzofuran, DPBF, (0.593 g, 2.19 mmol) and 2 (0.948 g, 5.71 mmol) were dissolved in chloroform (17.4 mL), and while shielded from light and under an argon atmosphere, the reaction mixture was stirred at room temperature for 24 h. The solvents were removed in vacuo, and the collected residue was dissolved in dry acetonitrile (8.0 mL). To the stirred solution was added BF₃·OEt₂ (2.0 mL, 16.3 mmol), and the reaction was refluxed under an argon atmosphere for 4 h. After the mixture was cooled, water was added to the reaction mixture, which resulted in formation of a yellow precipitate. This was collected by filtration, taken up in dichloromethane, washed with brine and water, and solvents removed in vacuo. Recrystallization from benzene gave 4 as a yellow crystalline solid (295 mg, 0.737 mmol, 34%). *R*_f (chloroform) = 0.70. ¹H NMR (400 MHz, CDCl₃): δ_H ppm 8.46 (s, 2H), 7.78 (m, 2H), 7.65 (m, 6H), 7.52 (m, 2H), 7.46 (m, 4H). ¹³C NMR (100 MHz, CDCl₃): δ_C ppm 163.4, 142.0, 137.1, 132.6, 131.1, 130.9, 129.1, 129.0, 128.8, 128.0, 127.8, 123.7. HRMS: [M + H]⁺ calcd for C₂₈H₁₆O₃, 401.1178; found, 401.1172.

1,3-Difluoro-2,4-dimethoxy-5-nitrobenzene (6). A sodium methoxide solution was prepared by adding sodium (2.2 equiv, 0.648 g, 28.2 mmol) to a flame-dried round bottomed flask containing MeOH (10.0 mL). Upon complete consumption of the sodium, the freshly prepared sodium methoxide solution was added dropwise to a stirred solution of commercially available 1,2,3,4-tetrafluoro-5-nitrobenzene (5), (2.50 g, 12.8 mmol), dissolved in MeOH (35 mL), and kept at 0 °C under an argon atmosphere. Thereafter, the reaction mixture was warmed to room temperature and left stirring for 4 h, with progress monitored by TLC. Upon completion, the reaction was quenched with an aqueous solution of citric acid (1 M), and MeOH was removed in vacuo. The resulting aqueous residue was taken up in Et₂O, washed twice with 1 M citric acid and brine, and dried over MgSO₄. Solvents were removed in vacuo to give a yellow oil. Purification by flash column chromatography (1:3 dichloromethane/pentane) yielded 1,3-difluoro-2,4-dimethoxy-5-nitrobenzene (6) (2.68 g, 12.21 mmol, 95%) as a yellow oil. *R*_f (1:3 dichloromethane/pentane) = 0.20. ¹H NMR (400 MHz, CDCl₃): δ_H ppm 7.51 (dd, *J* = 2.31, 11.0 Hz, 1H), 4.13 (t, *J* = 1.8 Hz, 3H), 4.01 (d, *J* = 1.2 Hz, 3H). ¹⁹F NMR (377 MHz, CDCl₃): δ_F ppm 131.9 (m, 1F), 141.8 (d, *J* = 7.0 Hz, 1F). ¹³C NMR (100 MHz, CDCl₃): δ_C ppm 149.5 (dd, *J* = 6.5 Hz, 248.0 Hz), 149.2 (dd, *J* = 5.4 Hz, 248.2 Hz), 142.1 (m), 141.0 (dd, *J* = 3.7 Hz, 13.9 Hz), 136.6 (m), 108.3 (dd, *J* = 3.5 Hz, 25.5 Hz), 63.0 (dd, *J* = 0.8 Hz, 4.3 Hz), 61.8 (t, *J* = 4.5 Hz). HRMS: [M + H]⁺ calcd for C₈H₇F₂NO₄, 220.0421; found, 220.0420. Our data are in accord with previously reported data.⁶⁴

3,5-Difluoro-2,4-dimethoxyaniline (7). To a stirred solution of (6) (1.63 g, 7.44 mmol) and ammonium formate (1.88 g, 29.8 mmol) in MeOH (15.0 mL), 10% Pd on activated carbon (0.245 g) was slowly added. The reaction mixture was stirred in an open flask while reaction progress was monitored by TLC analysis. After completion, the reaction mixture was filtered through Celite, and MeOH was removed in vacuo. The residue was taken up in water and extracted with dichloromethane three times. The combined organic fractions were dried over MgSO_4 , and solvents were removed in vacuo to yield pure 3,5-difluoro-2,4-dimethoxyaniline (7) as an oil (1.38 g, 7.29 mmol, 98%). ^1H NMR (400 MHz, CDCl_3): δ_{H} ppm 6.22 (dd, $J = 2.2$, 12.1 Hz, 1H), 3.82 (s, $J = 4.4$ Hz, 6H). ^{19}F NMR (377 MHz, CDCl_3): δ_{F} ppm 135.5 (m, 1F), 146.9 (s, 1F). ^{13}C NMR (100 MHz, CDCl_3): δ_{C} ppm 151.9 (dd, $J = 6.6$ Hz, 241.3 Hz), 149.9 (dd, $J = 7.9$ Hz, 245.7 Hz), 135.7 (m), 131.5 (m), 128.1 (m), 97.3 (dd, $J = 2.65$ Hz, 23.8 Hz), 62.1, 60.7 (d, $J = 4.41$ Hz). HRMS: $[\text{M} + \text{H}^+]$ calcd for $\text{C}_8\text{H}_7\text{F}_2\text{NO}_2$, 190.0680; found, 190.0693. Our data are in accord with previously reported data.⁶⁴

1,3-Difluoro-2,4-dimethoxybenzene (8). To a stirred solution, kept at 0 °C, of concentrated HCl (6.8 mL) and water (25.7 mL) was added 7 (2.185 g, 11.55 mmol). The reaction mixture was treated with a cold solution of sodium nitrite (0.831 g, 12.13 mmol) dissolved in water (6 mL). A solution of hypophosphorous acid (30.5 mL, 231 mmol, 50 wt % in water) was added slowly to the reaction, and it was left stirring at 5 °C overnight under an argon atmosphere. The reaction mixture was heated to room temperature and stirred for 2 h, after which it was diluted with water. The resulting mixture was extracted three times with dichloromethane, washed with brine, dried over MgSO_4 , filtered, and solvents removed in vacuo. The collected residue was purified by flash column chromatography (1:4 dichloromethane/pentane) to give 8 as a colorless oil (1.85 g, 10.6 mmol, 92%). R_{f} (1:4 dichloromethane/pentane) = 0.25. ^1H NMR (400 MHz, CDCl_3): δ_{H} ppm 6.79 (m, 1H), 6.56 (dt, $J = 4.6$ Hz, 8.9 Hz, 1H), 4.00 (s, 3H), 3.86–3.84 (m, 3H). ^{19}F NMR (377 MHz, CDCl_3): δ_{F} ppm 138.9 (m, 1F), 150.1 (m, 1F). ^{13}C NMR (100 MHz, CDCl_3): δ_{C} ppm 150.1 (dd, $J = 3.8$ Hz, 241.2 Hz), 146.1 (dd, $J = 5.5$ Hz, 247.6 Hz), 145.1 (dd, $J = 2.9$ Hz, 9.6 Hz), 137.4 (dd, $J = 11.5$ Hz, 26.8 Hz), 109.9 (dd, $J = 4.1$ Hz, 20.4 Hz), 106.2 (dd, $J = 2.0$ Hz, 8.6 Hz), 61.9 (t, $J = 3.5$ Hz), 56.8. HRMS: $[\text{M} + \text{H}^+]$ calcd for $\text{C}_8\text{H}_8\text{F}_2\text{O}_2$, 175.0571; found, 175.0575. Our data are in accord with previously reported data.⁶⁴

2,4-Difluorobenzene-1,3-diol (9). Compound 8 (1.167 g, 6.70 mmol) was dissolved in dry dichloromethane and stirred under an argon atmosphere at room temperature. BBr_3 (20.0 mL, 20.0 mmol, 1 M in dichloromethane) was slowly added to the solution via a syringe over 5 min. The reaction was left stirring at room temperature while progress was monitored by TLC analysis. After 48 h, water was slowly added to the reaction mixture and this was left stirring until all precipitates were dissolved. The suspension was extracted three times with dichloromethane, and the organic solvents were dried (MgSO_4) and removed in vacuo. The collected residue was purified by flash column chromatography (1:4 EtOAc/dichloromethane) giving (9) as a slightly red crystalline solid (0.881 g, 6.03 mmol, 90%). R_{f} (1:4 EtOAc/dichloromethane) = 0.25. ^1H NMR (400 MHz, CDCl_3): δ_{H} ppm 6.78 (dt, $J = 2.4$ Hz, 9.5 Hz, 1H), 6.49 (dt, $J = 5.0$ Hz, 9.1 Hz, 1H), 5.20 (broad s, 1H), 4.96 (broad s, 1H). ^{19}F NMR (377 MHz, CDCl_3): δ_{F} ppm 146.1 (m, 1F), 160.0 (m, 1F). ^{13}C NMR (100 MHz, CDCl_3): δ_{C} ppm 145.8 (dd, $J = 3.7$ Hz, 233.6 Hz), 140.8 (dd, $J = 4.9$ Hz, 235.1 Hz), 140.6 (dd, $J = 2.9$ Hz, 12.4 Hz), 133.2 (dd, $J = 13.2$ Hz, 18.2 Hz), 110.3 (dd, $J = 4.1$ Hz, 19.4 Hz), 106.6 (dd, $J = 1.1$ Hz, 7.7 Hz). HRMS: $[\text{M} + \text{H}^+]$ calcd for $\text{C}_6\text{H}_4\text{F}_2\text{O}_2$, 147.0258; found, 147.0261. Our data are in accord with previously reported data.⁶⁴

2',4',5',7'-Tetrafluoro-3',6'-dihydroxy-5,10-diphenyl-3H-spiro[anthra[2,3-c]furan-1,9'-xanthen]-3-one (10). Compound 9 (229 mg, 1.57 mmol) and compound 4 (135 mg, 0.337 mmol) were dissolved in methane sulfonic acid (1.6 mL, 25.6 mmol). The reaction mixture was heated to 150 °C, under argon atmosphere and light shielding, for 24 h. The cooled reaction mixture was poured into ice water, and the precipitate, containing ASG, was collected and dried. The solids were dissolved in acetic anhydride (4.0 mL, 42.4 mmol),

pyridine (2.0 mL, 24.7 mmol) was added, and the reaction was stirred for 10 min at room temperature under an argon atmosphere. Subsequently, the reaction was poured into 2% aqueous hydrochloric acid and extracted three times with dichloromethane. The combined organic fractions were washed with brine, dried over Na_2SO_4 , filtered, and solvents removed in vacuo. The resulting residue, containing the acetylated lactone form of ASG, was purified with flash column chromatography (dichloromethane) to give semipure 10 (120 mg).

9,10-Diphenyl-3-(2,4,5,7-tetrafluoro-6-hydroxy-3-oxo-3H-xanthen-9-yl)anthracene-2-carboxylic acid (ASG). The product mixture from the previous step (vide supra), containing 10, was dissolved in THF (10 mL), methanol (10 mL), and water (1.6 mL). Aqueous ammonia (25 vol %, 2.9 mL, 33.5 mmol) was added to the solution, and the deacetylation reaction was stirred while shielded from light under an argon atmosphere for 5 min at room temperature. The reaction mixture was filtered and diluted with water, and the pH was adjusted to ~2 with 10% hydrochloric acid. The organic solvents were removed in vacuo. The aqueous slurry was extracted with dichloromethane, dried over Na_2SO_4 , and solvents removed in vacuo giving a red residue. The mixture was purified using MPLC (Teledyne Isco CombiFlash Rf, column: C18 RediSep 28g, solvent A: 0.1% TFA in water, solvent B: acetonitrile, gradient 30% → 100% B, detection 214 nm). The desired compound eluted with a solvent mixture containing 65% B. Acetonitrile was removed in vacuo, and the pH of the aqueous layer was adjusted to ~2 with 10% hydrochloric acid and extracted three times with EtOAc. The combined organic fractions were dried with MgSO_4 , and solvents removed in vacuo to give ASG as a red solid (26 mg, 40 mmol, 12%). R_{f} (9:1:0.1 chloroform/methanol/acetic acid) = 0.25. ^1H NMR (400 MHz, acetone- d_6): δ_{H} ppm 8.46 (s, 1H) 7.80–7.60 (m, 8H), 7.55–7.45 (m, 5H), 7.41–7.37 (m, 2H), 6.58 (d, $J = 10.5$ Hz, 2H). ^{19}F NMR (377 MHz, acetone- d_6): δ_{F} ppm 135.3 (t, $J = 10.1$ Hz, 2F), 153.1 (d, $J = 8.8$ Hz, 2F). ^{13}C NMR (100 MHz, acetone- d_6): δ_{C} ppm 167.7, 147.8, 143.4, 142.1, 142.0, 140.6, 139.6, 138.3, 137.6, 137.1, 137.0, 136.9, 136.8, 136.7, 131.8, 131.7, 131.6, 131.2, 130.4, 129.6, 129.4, 129.0, 128.7, 127.3, 127.0, 123.9, 122.2, 110.3, 110.2, 109.2, 109.0. HRMS: $[\text{M} + \text{H}^+]$ calcd for $\text{C}_{40}\text{H}_{20}\text{F}_4\text{O}_5$, 657.1325; found, 657.1331.

■ ASSOCIATED CONTENT

Supporting Information

NMR spectra of the compounds prepared. This material is available free of charge via the Internet at <http://pubs.acs.org>.

■ AUTHOR INFORMATION

Corresponding Author

*E-mail: progilby@chem.au.dk.

Author Contributions

[†]S.K.P. and J.H. contributed equally to this work.

Notes

The authors declare no competing financial interest.

■ ACKNOWLEDGMENTS

This work was supported by the Danish National Research Foundation. The authors thank Mikkel Due Petersen for the gift of carboxy Oregon Green and 4', 5'-difluoro Oregon Green.

■ REFERENCES

- (1) Nagano, T. *J. Clin. Biochem. Nutr.* **2009**, *45*, 111–124.
- (2) Soh, N. *Anal. Bioanal. Chem.* **2006**, *386*, 532–543.
- (3) Gomes, A.; Fernandes, E.; Lima, J. L. F. C. *J. Biochem. Biophys. Methods* **2005**, *65*, 45–80.
- (4) Setsukinai, K.; Urano, Y.; Kakinuma, K.; Majima, H. J.; Nagano, T. *J. Biol. Chem.* **2003**, *278*, 3170–3175.
- (5) Lin, V. S.; Dickinson, B. C.; Chang, C. J. *Methods Enzymol.* **2013**, *526*, 19–43.

- (6) Halliwell, B.; Gutteridge, J. M. C. *Free Radicals in Biology and Medicine*, 3rd ed.; Oxford University Press: Oxford, U.K., 1999.
- (7) Paterson, M. J.; Christiansen, O.; Jensen, F.; Ogilby, P. R. *Photochem. Photobiol.* **2006**, *82*, 1136–1160.
- (8) Kanofsky, J. R. *Chem.-Biol. Interact.* **1989**, *70*, 1–28.
- (9) Klotz, L.-O.; Kröncke, K.-D.; Sies, H. *Photochem. Photobiol. Sci.* **2003**, *2*, 88–94.
- (10) Schweitzer, C.; Schmidt, R. *Chem. Rev.* **2003**, *103*, 1685–1757.
- (11) Ogilby, P. R. *Chem. Soc. Rev.* **2010**, *39*, 3181–3209.
- (12) Sawyer, D. T. *Oxygen Chemistry*; Oxford University Press: New York, 1991.
- (13) Clennan, E. L.; Pace, A. *Tetrahedron* **2005**, *61*, 6665–6691.
- (14) Redmond, R. W.; Kochevar, I. E. *Photochem. Photobiol.* **2006**, *82*, 1178–1186.
- (15) Silva, E. F. F.; Pedersen, B. W.; Breitenbach, T.; Toftgaard, R.; Kuimova, M. K.; Arnaut, L. G.; Ogilby, P. R. *J. Phys. Chem. B* **2012**, *116*, 445–461.
- (16) Skovsen, E.; Snyder, J. W.; Ogilby, P. R. *Photochem. Photobiol.* **2006**, *82*, 1187–1197.
- (17) Tanaka, K.; Miura, T.; Umezawa, N.; Urano, Y.; Kikuchi, K.; Higuchi, T.; Nagano, T. *J. Am. Chem. Soc.* **2001**, *123*, 2530–2536.
- (18) Song, B.; Wang, G.; Tan, M.; Yuan, J. *J. Am. Chem. Soc.* **2006**, *128*, 13442–13450.
- (19) Hideg, E. *Cent. Eur. J. Biol.* **2008**, *3*, 273–284.
- (20) Ragàs, X.; Jiménez-Banzo, A.; Sanchez-Garcia, D.; Batllori, X.; Nonell, S. *Chem. Commun.* **2009**, 2920–2922.
- (21) Xu, K.; Wang, L.; Qiang, M.; Wang, L.; Li, P.; Tang, B. *Chem. Commun.* **2011**, *47*, 7386–7388.
- (22) Kim, S.; Fujitsuka, M.; Majima, T. *J. Phys. Chem. B* **2013**, *117*, 13985–13992.
- (23) Ruiz-Gonzalez, R.; Zanicco, R.; Gidi, Y.; Zanicco, A. L.; Nonell, S.; Lemp, E. *Photochem. Photobiol.* **2013**, *89*, 1427–1432.
- (24) Gollmer, A.; Arnbjerg, J.; Blaikie, F. H.; Pedersen, B. W.; Breitenbach, T.; Daasbjerg, K.; Glasius, M.; Ogilby, P. R. *Photochem. Photobiol.* **2011**, *87*, 671–679.
- (25) Lin, H.; Shen, Y.; Chen, D.; Lin, L.; Wilson, B. C.; Li, B.; Xie, S. *J. Fluoresc.* **2013**, *23*, 41–47.
- (26) Li, X.; Zhang, G.; Ma, H.; Zhang, D.; Li, J.; Zhu, D. *J. Am. Chem. Soc.* **2004**, *126*, 11543–11548.
- (27) Song, D.; Cho, S.; Han, Y.; You, Y.; Nam, W. *Org. Lett.* **2013**, *15*, 3582–3585.
- (28) Singlet Oxygen Sensor Green (SOSG) Product Information. Molecular Probes/Invitrogen/Life Technologies. Available at: <http://www.invitrogen.com>.
- (29) Ueno, T.; Urano, Y.; Setsukinai, K.; Takakusa, H.; Kojima, H.; Kikuchi, K.; Ohkubo, K.; Fukuzumi, S.; Nagano, T. *J. Am. Chem. Soc.* **2004**, *126*, 14079–14085.
- (30) Urano, Y.; Kamiya, M.; Kanda, K.; Ueno, T.; Hirose, K.; Nagano, T. *J. Am. Chem. Soc.* **2005**, *127*, 4888–4894.
- (31) Mottram, L. F.; Boonyarattanakalin, S.; Kovel, R. E.; Peterson, B. R. *Org. Lett.* **2006**, *8*, 581–584.
- (32) Mottram, L. F.; Maddox, E.; Schwab, M.; Beaufils, F.; Peterson, B. R. *Org. Lett.* **2007**, *9*, 3741–3744.
- (33) Sun, W.-C.; Gee, K. R.; Klaubert, D. H.; Haugland, R. P. *J. Org. Chem.* **1997**, *62*, 6469–6475.
- (34) Lakowicz, J. R. *Principles of Fluorescence Spectroscopy*, 3rd ed.; Springer: New York, 2006.
- (35) Ogilby, P. R.; Foote, C. S. *J. Am. Chem. Soc.* **1983**, *105*, 3423–3430.
- (36) deWit, J. N.; Klanrenbeek, G. *J. Dairy Sci.* **1984**, *67*, 2701–2710.
- (37) Kristiansen, M.; Scurlock, R. D.; Lu, K.-K.; Ogilby, P. R. *J. Phys. Chem.* **1991**, *95*, 5190–5197.
- (38) McGarvey, D. J.; Wilkinson, F.; Worrall, D. R.; Hopley, J.; Shaikh, W. *Chem. Phys. Lett.* **1993**, *202*, 528–534.
- (39) Flors, C.; Ogilby, P. R.; Luis, J. G.; Grillo, T. A.; Izquierdo, L. R.; Gentili, P.-L.; Bussotti, L.; Nonell, S. *Photochem. Photobiol.* **2006**, *82*, 95–103.
- (40) Jensen, P.-G.; Arnbjerg, J.; Tolbod, L. P.; Toftgaard, R.; Ogilby, P. R. *J. Phys. Chem. A* **2009**, *113*, 9965–9973.
- (41) Nielsen, C. B.; Johnsen, M.; Arnbjerg, J.; Pittelkow, M.; McIlroy, S. P.; Ogilby, P. R.; Jørgensen, M. *J. Org. Chem.* **2005**, *70*, 7065–7079.
- (42) Nielsen, C. B.; Arnbjerg, J.; Johnsen, M.; Jørgensen, M.; Ogilby, P. R. *J. Org. Chem.* **2009**, *74*, 9094–9104.
- (43) Morrow, G. W. In *Organic Electrochemistry*, 4th ed.; Lund, H., Hammerich, O., Eds.; Marcel Dekker: New York, 2001; pp 589–620.
- (44) Wilkinson, F.; Helman, W. P.; Ross, A. B. *J. Phys. Chem. Ref. Data* **1995**, *24*, 663–1021.
- (45) Umezawa, N.; Tanaka, K.; Urano, Y.; Kikuchi, K.; Higuchi, T.; Nagano, T. *Angew. Chem., Int. Ed.* **1999**, *38*, 2899–2901.
- (46) Donyagina, V. F.; Kovshev, E. I.; Luk'yanets, E. A. *Russ. J. Gen. Chem.* **2006**, *76*, 654–658.
- (47) Magde, D.; Wong, R.; Seybold, P. G. *Photochem. Photobiol.* **2002**, *75*, 327–334.
- (48) Wilkinson, F.; Helman, W. P.; Ross, A. B. *J. Phys. Chem. Ref. Data* **1993**, *22*, 113–262.
- (49) Gudgin Dickson, E. F.; Kennedy, J. C.; Pottier, R. H. In *Photodynamic Therapy*; Patrice, T., Ed.; Royal Society of Chemistry: Cambridge, 2003; p 81–103.
- (50) Gollmer, A.; Besostri, F.; Breitenbach, T.; Ogilby, P. R. *Free Radical Res.* **2013**, *47*, 718–730.
- (51) Johnson, L. V.; Walsh, M. L.; Chen, L. B. *Proc. Natl. Acad. Sci. U.S.A.* **1980**, *77*, 990–994.
- (52) Heggeness, M. H.; Simon, M.; Singer, S. J. *Proc. Natl. Acad. Sci. U.S.A.* **1978**, *75*, 3863–3866.
- (53) Breitenbach, T.; Kuimova, M. K.; Gbur, P.; Hatz, S.; Schack, N. B.; Pedersen, B. W.; Lambert, J. D. C.; Poulsen, L.; Ogilby, P. R. *Photochem. Photobiol. Sci.* **2009**, *8*, 442–452.
- (54) Hatz, S.; Poulsen, L.; Ogilby, P. R. *Photochem. Photobiol.* **2008**, *84*, 1284–1290.
- (55) Bosio, G. N.; Breitenbach, T.; Parisi, J.; Reigosa, M.; Blaikie, F. H.; Pedersen, B. W.; Silva, E. F. F.; Martire, D. O.; Ogilby, P. R. *J. Am. Chem. Soc.* **2013**, *135*, 272–279.
- (56) Salice, P.; Arnbjerg, J.; Pedersen, B. W.; Toftgaard, R.; Beverina, L.; Pagani, G. A.; Ogilby, P. R. *J. Phys. Chem. A* **2010**, *114*, 2518–2525.
- (57) Keszthelyi, T.; Weldon, D.; Andersen, T. N.; Poulsen, T. D.; Mikkelsen, K. V.; Ogilby, P. R. *Photochem. Photobiol.* **1999**, *70*, 531–539.
- (58) Arnbjerg, J.; Johnsen, M.; Frederiksen, P. K.; Braslavsky, S. E.; Ogilby, P. R. *J. Phys. Chem. A* **2006**, *110*, 7375–7385.
- (59) Pimenta, F. M.; Jensen, R. L.; Holmegaard, L.; Esipova, T. V.; Westberg, M.; Breitenbach, T.; Ogilby, P. R. *J. Phys. Chem. B* **2012**, *116*, 10234–10246.
- (60) Hatz, S.; Lambert, J. D. C.; Ogilby, P. R. *Photochem. Photobiol. Sci.* **2007**, *6*, 1106–1116.
- (61) Edelstein, A.; Amodaj, N.; Hoover, K.; Vale, R.; Stuurman, N. *Curr. Protoc. Mol. Biol.* **2010**, *92*, 1–17.
- (62) Nonell, S.; Gonzalez, M.; Trull, F. R. *Afinidad* **1993**, *448*, 445–450.
- (63) Goh, Y. W.; Pool, B. R.; White, J. M. *J. Org. Chem.* **2008**, *73*, 151–156.
- (64) Hedberg, C.; Dekker, F. J.; Rusch, M.; Renner, S.; Wetzel, S.; Vartak, N.; Gerding-Reimers, C.; Bon, R. S.; Bastiaens, P. I. H.; Waldmann, H. *Angew. Chem., Int. Ed.* **2011**, *50*, 9832–9837.